# Out-of-Band Fiber-Optic Time and Frequency Transfer Using Asymmetric and Symmetric Opto-Electronic Repeaters

Thomas Fordell, K. Hanhijärvi, A. E. Wallin, J. Myyry, and T. Lindvall

***Abstract*—Signal repeaters for fiber-optic communication can be realized with back-to-back connected transceivers. This configuration can provide high gain (≈30 dB) at low cost, and the needed semiconductor lasers and modulators can be realized for practically any relevant wavelength. Unfortunately, for time and frequency (TF) transfer the uncorrelated wavelength drifts in the transceiver lasers can compromise transfer stability, and device replacement due to failure may result in large time offsets that have to be measured via global navigation satellite services (GNSS). This work demonstrates that good results can nevertheless be obtained with standard telecom dense wavelength-division multiplexing (DWDM) transceivers over long time periods (years). More importantly, a simple wavelength-symmetric repeater is proposed that can be used to cancel the detrimental effects of wavelength drifts and which lessens the need for link recalibrations after transceiver replacements. In a proof-of-concept test setup, timing drift due to wavelength drift of a repeater laser is reduced by approximately two orders of magnitude.**

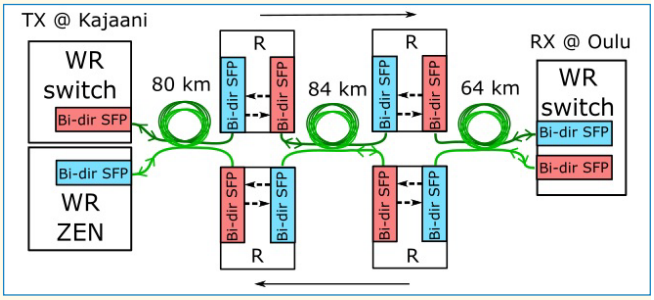


***Index Terms*—Fiber optics, synchronization, time and frequency (TF) transfer.**

## I. Introduction

COMPARED with global navigation satellite services (GNSS), fiber-optic long-haul time and frequency (TF) transfer can provide better security against jamming and spoofing as well as much higher performance in terms of both stability and accuracy.

To reduce cost and increase availability, operating outside the conventional telecom band ($C$-band) is interesting [1], [2], especially since this enables easy bypass of normal telecom equipment that use separate fibers for the up- and downlink. For accurate TF transfer, symmetry in the link delay between the uplink and the downlink is essential, and having separate fibers means that noise due to temperature variations and vibrations is not as well correlated. More importantly, maintenance work might change the length difference between the two fibers [3], [4] resulting in a need to recalibrate the link with, e.g., GNSS. Operating outside the data traffic bands also means that both the fibers can be used bidirectionally, that is, the signal can be looped back to the transmitter for verification.

In the updated Finnish university network (FUNET), a 13-nm-wide band for bidirectional TF signals has been allocated around 1610 nm (see Fig. 1). Coherent optical transmission is used for the data in the $C$-band; therefore, the network consists entirely of standard single-mode fiber without chromatic dispersion compensation. On the short wavelength side is the optical supervisory channel (OSC) and high-power Raman pumps. Optical time-domain reflectometry and link monitoring is performed around 1650 nm, which leaves wavelengths in the $L$-band available for timing signals.

For long-haul links, the timing signals need to be amplified. Brillouin amplifiers have been used successfully for optical frequency transfer [6], but the very narrow gain bandwidth (≈10 MHz) makes them unsuitable for modulated timing signals that typically require much larger bandwidths to achieve high precision. The polarization dependence of the gain is also problematic. Raman amplification around 1610 nm is not an option in the present case since the wavelength of the required high-power pump is incompatible with the rest of the currently used optical line system devices, which support Raman amplification only in the $C$-band and not in the $C + L$-band. The remaining alternatives are $L$-band EDFAs and semiconductor solutions. The considered wavelengths are

Manuscript received 3 February 2023; accepted 19 April 2023. Date of publication 28 April 2023; date of current version 28 June 2023. This work was supported by the Academy of Finland under Decision 339821. The work is also part of the Academy of Finland Flagship Programme, Photonics Research and Innovation (PREIN), Decision 320168. *(Corresponding author: Thomas Fordell.)*

Thomas Fordell, K. Hanhijärvi, A. E. Wallin, and T. Lindvall are with VTT Technical Research Centre of Finland Ltd., National Metrology Institute VTT MIKES, 02044 Espoo, Finland (e-mail: thomas.fordell@vtt.fi).

J. Myyry is with CSC-IT Center for Science Ltd., 02150 Espoo, Finland.

Digital Object Identifier 10.1109/TUFFC.2023.3271371

### Highlights

- **A 2 × 228-km single-fiber time transfer link in the L-band is presented that utilizes back-to-back connected telecom transceivers for signal amplification.**
- **Symmetric opto-electronic repeaters are proposed that reduce the timing drift caused by transceiver wavelength drift and which lessen the need for link re-calibration after transceiver replacements.**
- **The high gain, wide wavelength range and potentially high performance of integrated, symmetric opto-electronic repeaters facilitate wider availability of precision fiber-optic timing solutions.**

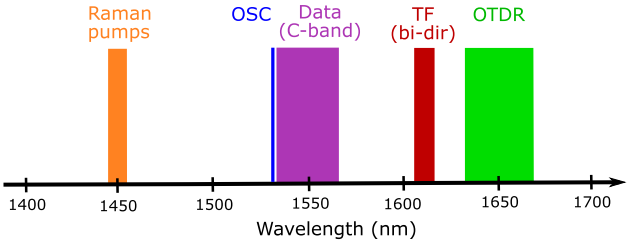


Fig. 1. Wavelength allocations in the FUNET. A similar structure is used in the SUNET [5]. OSC: optical supervisory channel. TF: time and frequency. OTDR: optical time-domain reflectometry.

inside the bandwidth of bidirectional $L$-band EDFAs [2], and they would be the best choice especially for transferring optical TF references although the gain cannot be increased beyond ≈20 dB due to the onset of amplifier instabilities. Operating close to the maximum gain might require continuous amplifier state monitoring [7].

Semiconductor optical amplifiers are available for a very wide wavelength range, but they suffer from higher noise figures, polarization dependence, and, especially, severe nonlinearities that make them not very attractive for the present application [8]. Instead, in this work, the 228-km fiber link uses two repeater stations that use semiconductor opto-electronic 2R (Reamplification, Reshaping) repeaters based on 1605- and 1615-nm small form-factor pluggable (SFP) telecom transceivers. The advantages of this approach are the low cost of the transceivers, high gain without amplifier instabilities, and the inherent reshaping of signals (2R regeneration). Similar repeaters are used for time transfer in the 440-km-long timing link between Stockholm and Sundsvall in the Swedish University Network (SUNET) [5].

As will be shown in Section II, such low-cost opto-electronic repeaters can, in a White Rabbit (WR) [9] network, provide timing accuracy well below 1 ns over hundreds of kilometers and over long time spans (years). A considerable vulnerability of this amplification solution is, however, timing drift due to uncorrelated wavelength drift in the SFP transceivers. To lessen the impact of wavelength drift, Section III presents a proof-of-concept wavelength-symmetric signal repeater that can reduce the wavelength-induced timing drift by two orders of magnitude.

WR was used in this work due to commercially available hardware, low-cost, ease of use, and a performance suitable not only for industrial but also for scientific applications. Considerable effort has been put into developing absolute calibration procedures for WR links, including mitigating

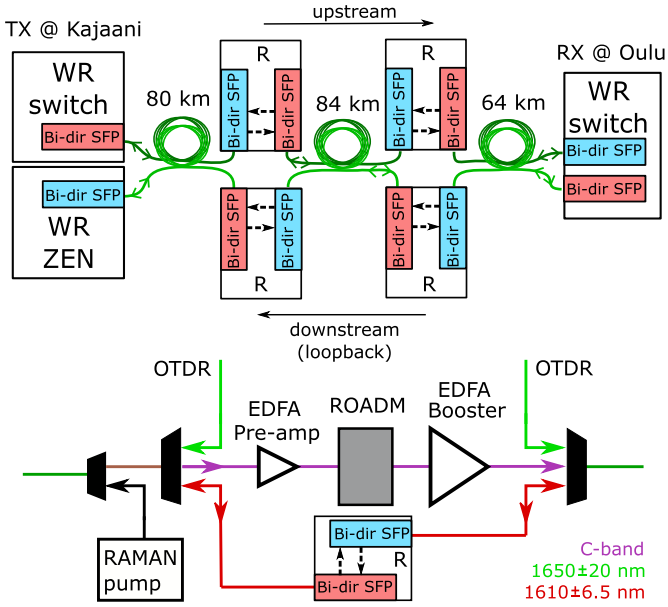


Fig. 2. Top: Schematics of the WR link with two repeater stations (R) based on bidirectional SFP transceivers (1605 and 1615 nm). Bottom: Schematics of the optical connections at a repeater station. OTDR: optical time-domain reflectometry. ROADM: reconfigurable optical add-drop multiplexer. WDM: wavelength-division multiplexer.

the effect of link propagation asymmetry [10], [11]. The symmetric repeater presented below also reduces the problem of wavelength-dependent/dispersive asymmetry. It is important to note, however, that the symmetric repeater scheme is not specific to WR networks.

## II. 2 × 228 km WR Link Using Asymmetric 2R Repeaters

A schematic of the Kajaani–Oulu–Kajaani 2 × 228 km WR fiber link is shown in Fig. 2 (top). Two regenerative opto-electronic repeater stations are used bidirectional SFP transceivers (ADVA BC1615V and BC1605V) on CTC FRM220-1000DS repeater boards. The frequency stability of the transceivers is specified as 12 GHz (≈0.1 nm) to end of life. The lower part of Fig. 2 shows a general overview of the optical connections at the sites.

The results for the looped back time transfer signal over a time span of 21 months are shown in Fig. 3(a). The yellow trace gives the difference in 1-pulse-per-second signals between the two WR devices in Kajaani measured every minute with a time interval counter (Keysight 53230A) as a

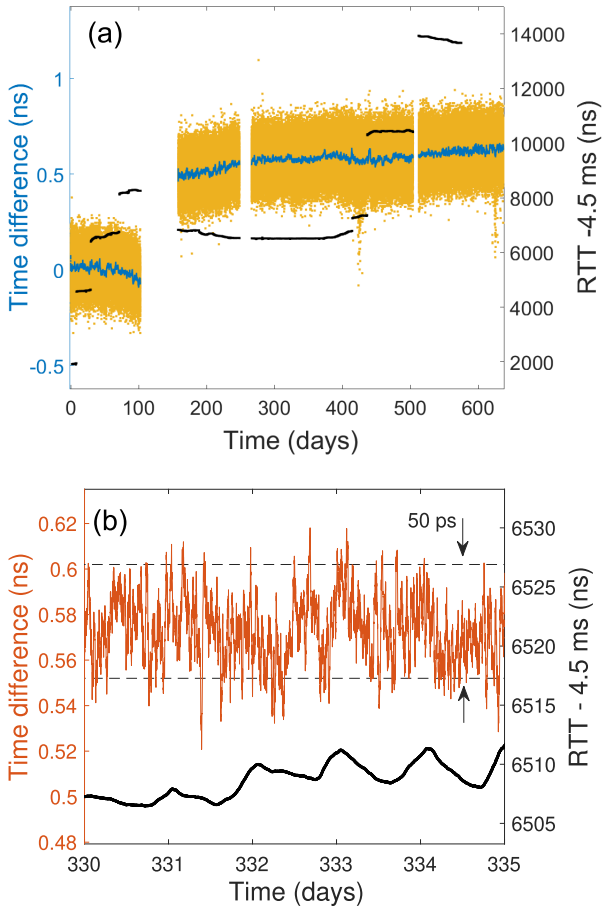


Fig. 3. (a) Timing drift over 21 months of the looped back signal (2 × 228 km). The 1-min readings (yellow) are measured as a double difference between the receiver, the transmitter, and a Cs clock. A one-day running average is shown in blue, and the black curve indicates the Kajaani–Oulu–Kajaani RTT that is plotted as two times the Kajaani–Oulu RTT as measured by the WR-ZEN node in Kajaani. (The RTT data contain gaps also due to data acquisition issues.) (b) Zoom-in of a five-day interval that shows intraday variations with 1-h averaging.

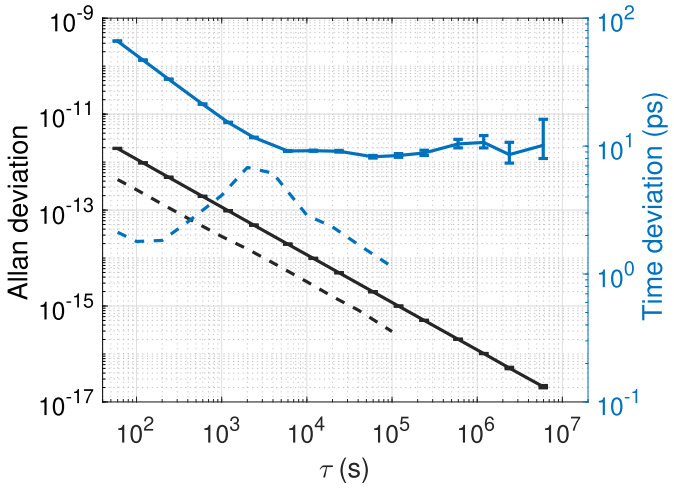


Fig. 4. Allan deviation and time deviation for the 2 × 228 km = 456 km link within the time interval 158 days < $t$ < 637 days [yellow trace in Fig. 3(a)]. The dashed lines indicate estimates for the measurement system noise floor.

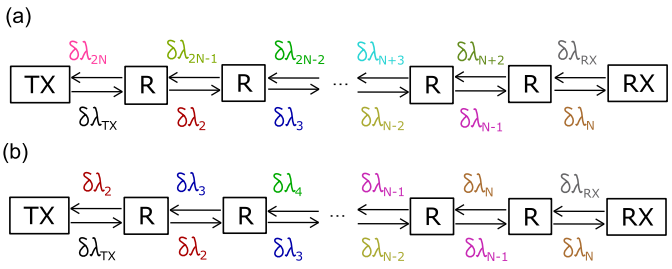


Fig. 5. (a) TF transfer using traditional asymmetric opto-electronic 2R repeaters as used in the Kajaani–Oulu–Kajaani link (see Fig. 2). The wavelength drift of the two transceivers in each repeater (R) is marked by $\delta\lambda_i$. (b) In a symmetric repeater, the same light source is used in both the directions, resulting in equal wavelength variations in the two directions.

double difference between the two switches and a Cs clock. The blue trace is a one-day moving average. Also shown is the Kajaani–Oulu–Kajaani round-trip time (RTT, black), which is plotted as two times the Kajaani–Oulu RTT as measured by the WR-ZEN node in Kajaani. A zoomed-in view of a five-day interval with 1-h averaging in Fig. 3(b) reveals the typical intraday behavior.

The large data gap and the resulting time offset between $t = 102$ and 158 days are due to technical problems that occurred during this time that rendered the data unreliable. Following the replacement of one of the WR switches with one running newer firmware on $t = 158$ days, the link performance has been good. (The resulting offset could, of course, be easily adjusted to zero.) The timing drift is about −80 ps during the first 102 days and +140 ps during the last 16 months.

Fig. 4 shows the Allan deviation and time deviation for the raw data [yellow trace in Fig. 3(a)] computed using the Stable32 program. Due to the large gap and the uncorrected offset in the early part, only data for $t > 158$ days were used in the computation and the remaining small gaps were filled by interpolation. It should be noted that neither the Allan nor the time deviation is sensitive to a constant time drift (frequency offset), and so the small but clear overall drift in the time difference in Fig. 3 is not reflected in Fig. 4.

Fig. 3(a) also shows that the RTT (black) has changed considerably due to network maintenance and line fiber rerouting. Nevertheless, the time transfer has been largely unaffected since the single-fiber solution maintains symmetry between the uplink and the downlink when fiber is added or removed, contrary to the case when the uplink and the downlink use separate fibers [3] as normally done in fiber-optic networks.

While the results are satisfactory, a significant weakness of the link is that without loop-back or GNSS monitoring, there is no way of knowing if a possible wavelength drift in any one of the many transceivers is compromising transfer accuracy. Indeed, this is a plausible reason for the observed slow drift. In Section III, a wavelength-symmetric repeater is proposed to remedy this issue.

## III. Symmetric 2R Repeaters: A Proof of Concept

A general picture of a TF transfer link using opto-electronic repeaters is shown in Fig. 5, where the wavelength variations in each transceiver are indicated. Ignoring, e.g., polarization dependence and minor contributions from the link asymmetry

parameter $\alpha \approx 4 \cdot 10^{-5}$ [12], the resulting time variation in the receiver can be expressed as

$$\delta t_{\mathrm{RX}} = \frac{1}{2}\left[\overline{D}_{N+1}L_{N+1}\delta\lambda_{\mathrm{RX}} - \overline{D}_1 L_1 \delta\lambda_{\mathrm{TX}} + \sum_{i=2}^{N}(\overline{D}_{i+N}L_{i+N}\delta\lambda_{i+N} - \overline{D}_i L_i \delta\lambda_i)\right] \quad (1)$$

where $\delta\lambda_{\mathrm{TX}}$, $\delta\lambda_{\mathrm{RX}}$, and $\delta\lambda_i$ are the wavelength drifts of the transmitter, the receiver, and the repeaters, respectively. $L_i$ are the various fiber lengths associated with $\delta\lambda_i$, and since $\delta\lambda_i$ and $\delta\lambda_{2N+1-i}$ travel the same path albeit in opposite directions, $L_i = L_{2N+1-i}$. The effective fiber dispersion $\overline{D}_i$ is defined via

$$\overline{D}_i L_i = \sum_j D_{ij} L_{ij} \quad (2)$$

that is, $\overline{D}_i$ takes into account that in a dispersion managed network, each leg with a total distance $L_i$ may be composed of a number of different fibers with length $L_{ij}$ and dispersion $D_{ij}$. The dispersion temperature dependence is of the order of 1 fs/nm/km/K [13], [14] and can be ignored in the present context. In principle then, if $\overline{D}_i = 0$ for all $i$, that is, the link is perfectly dispersion compensated, then $\delta t_{\mathrm{RX}} = 0$ and the link is insensitive to wavelength variations. This is not a very practical approach and in modern coherent networks as used in Section II, fiber dispersion management is not needed and the link consists entirely of standard single-mode fiber. At 1610 nm, the dispersion is around 19 ps/nm/km, and if all the transceivers drift, say, 10 GHz, then the worst case drift is 0.4 ns. What the drift will be in practice depends, of course, on the type of transceivers used and the environmental and electrical changes they are subjected to.

The situation can be improved considerably with a wavelength-symmetric repeater [see Fig. 5(b)] where only one laser is used so that the wavelength variations are the same in both the directions. Thus, $\delta\lambda_{2N+2-i} = \delta\lambda_i$ and the expression reduces to

$$\delta t_{\mathrm{RX}} = \frac{1}{2}\left[\overline{D}_{N+1}L_{N+1}\delta\lambda_{\mathrm{RX}} - \overline{D}_1 L_1 \delta\lambda_{\mathrm{TX}} + \sum_{i=2}^{N}(\overline{D}_{i-1}L_{i-1} - \overline{D}_i L_i)\delta\lambda_i\right]. \quad (3)$$

This implies that if the condition $\overline{D}_{i-1}L_{i-1} = \overline{D}_i L_i$ can be satisfied, then the timing drift due to wavelength drift in the repeaters can be largely suppressed. In a coherent network with a single fiber type, the condition is reduced to $L_{i-1} = L_i$.

To demonstrate this, a 2 × 25-km WR time transfer link was set up using a single symmetrical repeater built using discrete components, including a distributed feedback (DFB) laser (1533 nm) and two electro-optic Mach–Zehnder amplitude modulators (see Fig. 6). To test the wavelength sensitivity of the time transfer, the DFB laser was operated in a constant power mode and its temperature setpoint was slowly changed in a sinusoidal pattern, resulting in a peak-to-peak wavelength change of 2.6 nm, which corresponds to roughly three ITU channels and is significantly larger than the 0.1-nm wavelength

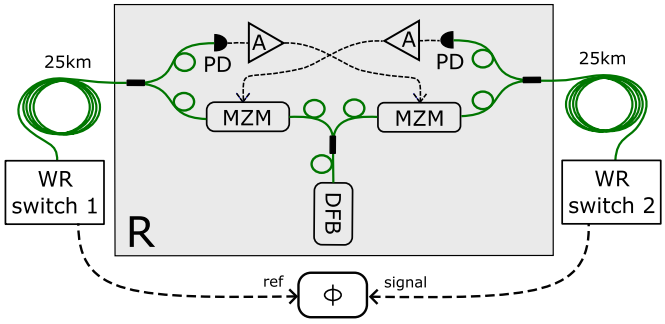


Fig. 6. Setup for testing wavelength drift sensitivity of a symmetric repeater (R) using two WR switches and a Symmetricom 3120A phase noise test probe (Φ). Light from a DFB laser is split into two Mach–Zehnder modulators (MZMs) that are driven by the amplified (A) output of the SFP transceiver modules, which are indicated here only as photodetectors (PDs).

stability of the SFP transceivers mentioned earlier. The reason behind the use of such a large scan range will become clear below. Switching to the asymmetric case could be easily done by feeding one of the modulators with an auxiliary DFB laser (not shown in Fig. 6).

In the asymmetric case with only one repeater ($N = 1$), the timing drift of the receiver due to wavelength drift in one of the repeater outputs, say $\delta\lambda_2$, is

$$\delta t_{\mathrm{RX}}^{\mathrm{asym}} = -\frac{DL_2}{2}\delta\lambda_2. \quad (4)$$

For a wavelength-symmetric repeater (Fig. 5(b) with $N = 1$), the corresponding timing drift is

$$\delta t_{\mathrm{RX}}^{\mathrm{sym}} = -\frac{D\delta\lambda_2}{2}\Delta L = \frac{\Delta L}{L_2} t_{\mathrm{RX}}^{\mathrm{asym}} \quad (5)$$

where $\Delta L = L_2 - L_1$. If $L_1 = L_2 = 25$ km, $D \approx 16$ ps/nm/km, and $\delta\lambda_2 = 2.6$ nm, then $\delta t_{\mathrm{RX}}^{\mathrm{asym}} \approx 520$ ps and $\delta t_{\mathrm{RX}}^{\mathrm{sym}} \approx 0$ ps are expected in the asymmetric and symmetric cases, respectively.

The results are shown in Fig. 7. In the asymmetric case, the receiver peak-to-peak timing drift, measured with a Microsemi 3120A phase meter, is 510 ps, in agreement with (4). In the symmetric case, the timing drift is reduced to 29 ps, but still some drift remains. A similar behavior was observed with different tuning speeds and also using a laser and modulators in the $O$-band (1347 nm). Adding a polarization scrambler to mitigate polarization mode dispersion [15] also had little effect. Power-level changes due to wavelength-dependent losses in the components and phase shifts in the modulators were also ruled out as possible causes.

What remains, then, is a problem in the WR phase compensation, that is, the output phase depends on the total link delay. In a perfect system, any delay changes would be fully corrected, and the output phase would be independent of the total link delay. To test this, a manual free-space delay stage was added to the link (not shown in Fig. 6). With the repeater wavelength kept constant, a change in the position of the delay line should not affect the time transfer, but as can be seen in the inset in Fig. 7, for some positions of the delay stage, a movement of roughly 11 cm resulted, after a transient, in an offset of ≈23 ps. The inset shows that the offset

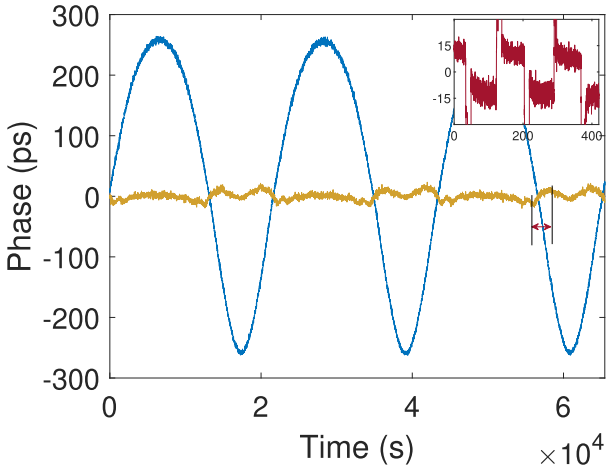


Fig. 7. Timing drift of the receiver as the wavelength of the DFB laser is tuned by varying its temperature while maintaining constant output power (yellow). In the asymmetric case (blue), an auxiliary DFB laser with constant wavelength is used to feed one of the modulators in Fig. 6. When a free-space delay line was added to the link, a delay change corresponding to that indicated by the red arrow caused a large time transfer offset (inset). This indicates that most if not all the drift remaining in the symmetric case (yellow) are due to the WR devices and are not due to the repeater configuration under test.

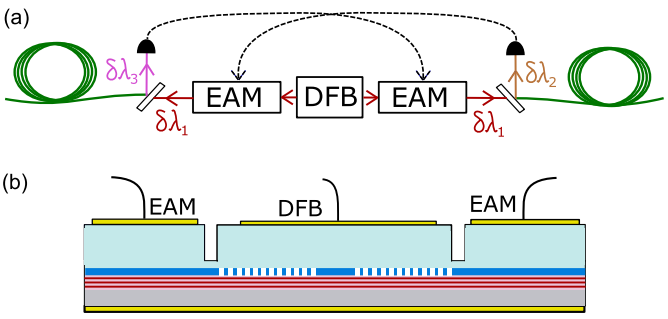


Fig. 8. (a) Example realization of a wavelength-symmetric repeater based on a DFB laser and dual EAMs. A wavelength locker (not shown) can also be added to one of the outputs. (b) Integrated structure with *C*-band DFB laser and two EAMs according to [16].

was repeatable and well above the short-term noise floor. The 11-cm movement corresponds to an RTT change of 730 ps, which, in turn, corresponds to a wavelength change of 0.96 nm for the laser in the symmetric repeater. Knowing the scanning speed, this value can be related to a (wall clock) time interval and is marked by the red arrow. This interval is approximately equal to the distance between the minimum and maximum time drifts and indicates that most, if not all, residual drift in Fig. 7 is due to a nonideal phase compensation of the WR switches and it is not due to the repeater configuration under test.

This phase compensation issue together with the short fiber lengths (25 km) used in the demonstration explains the need for the wide wavelength scan: a large delay change was needed to make the effect stand out. Using another time transfer technique or perhaps more optimized parameters for the WR switches should improve the result considerably. The long settling time seen in the inset is partly the reason for the use of such a low modulation frequency (46 $\mu$Hz) in Fig. 7. A significantly higher frequency would not give enough time for the WR devices to fully settle during the wavelength scan, compromising the measurement further. Furthermore, it is the effects of a slow drift that are interesting here, so a slow modulation was appropriate.

## IV. Discussion

The results in Section III are encouraging, but the component costs of the test setup are at least an order of magnitude higher than for the repeaters based on SFP dense wavelength-division multiplexing (DWDM) transceivers used in Section II. Fortunately, there are solutions: the repeater can, e.g., be realized by placing a DFB laser between two electro-absorption modulators [EAMs, Fig. 8(a)]. Such structures have already been grown for reducing the size and cost in multilane polarization-multiplexed communication systems: in [16], a $C$-band DFB laser with a $\lambda/4$-phase-shifted grating provided symmetric power output to two independent EAMs [see Fig. 8(b)]. The dual EAM structure required no extra processing steps, and a $2 \times 56$ GB/s nonreturn-to-zero modulation was demonstrated, far above the 1 GB/s used by the current and proposed 10-GB/s WR devices [17]. A grating- or etalon-based wavelength locker can be added after one of the outputs to stabilize the wavelength. An interesting additional feature of a symmetric repeater would be the possibility to modulate the wavelength at a frequency unique to each module. This way any repeater section that is not in balance could be detected as a modulation of the output of the receiver.

An alternative to the dual electro-absorption-modulated laser (EML) is to, e.g., split the front (main) output of a DFB laser into two modulators leaving the rear output available for, e.g., wavelength stabilization. Another option is to use two regular EML devices and to lock them to the same wavelength locker, although this might compromise stability. Frequency (or phase) locking of two EMLs could also be accomplished, e.g., by optical injection or by stabilizing their difference frequency via frequency counting or a frequency discriminator [18].

An important thing to note is that since the symmetric repeater reduces the timing drift due to wavelength changes, it also means that timing shift due to hardware replacements is reduced. In the asymmetric case, replacing the transceivers due to, e.g., device failures, might require recalibration of the entire link. Not so in the symmetric case if the link is balanced and the electro-optic and opto-electronic conversion delays are similar (or negligible).

Without dispersion compensation, if the length difference $\Delta L = L_i - L_{i-1}$ between fibers is small compared with $L_i, L_{i-1}$, then the timing drift in a symmetric repeater is suppressed by a factor $\gamma \approx 2\Delta L/(L_1 + L_2)$. In a link with one repeater and, say, 80- and 90-km fibers, $\gamma \approx 0.12$. If the length difference is reduced to 1 km (89 km + 90 km), then $\gamma \approx 0.01$. An important thing to note is that the requirement $L_{i-1} \approx L_i$ means that since fiber connections can usually only be made longer by adding spooled fiber at the repeaters, each leg must be made as long as the longest leg. This can be quite impractical especially when using existing fiber installations. In practice, a compromise would be needed.

Using also dispersion compensating fiber spools or fiber-Bragg gratings before and/or after the repeaters, as often done in dispersion managed networks, would make it easier to satisfy $\overline{D}_{i-1}L_{i-1} = \overline{D}_i L_i$. Since the effective dispersion does not need to be zeroed but only managed to an equal, nonzero level, the amount of dispersion compensation needed is relaxed considerably from having $\overline{D}_i = 0$ as long as the (in-coherent) bit rates are kept low enough [19].

Finally, it should be noted that the application of the proposed symmetric repeaters is not limited to WR networks; rather, the scheme should be viewed as a general method for signal amplification in cases where symmetry of the up- and downlink is important.

## V. Conclusion

An effective and simple signal repeater scheme for canceling the detrimental effect of laser wavelength drifts to fiber-optic TF transfer links was presented. The proof-of-concept table-top setup can be replaced by proven, integrated semiconductor structures and micro-optics; therefore, low-cost, compact, high-gain signal repeaters suitable for accurate and stable long-haul synchronization can be realized for virtually any practical wavelength band. The scheme also reduces the need for link recalibration after hardware replacements.

## References


[1] M. Cizek et al., "Coherent fibre link for synchronization of delocalized atomic clocks," *Opt. Exp.*, vol. 30, no. 4, pp. 5450–5464, Feb. 2022, doi: 10.1364/OE.447498.

[2] J. Vojtech et al., "Large scale infrastructure for precise time and frequency bidirectional transmission," in *Proc. 29th Infr. Remote Sens. Instrum.*, vol. 11830, M. Strojnik, Ed. Bellingham, WA, USA: SPIE, 2021, pp. 1–6, doi: 10.1117/12.2592328.

[3] E. F. Dierikx et al., "White rabbit precision time protocol on long-distance fiber links," *IEEE Trans. Ultrason., Ferroelectr., Freq. Control*, vol. 63, no. 7, pp. 945–952, Jul. 2016, doi: 10.1109/TUFFC.2016.2518122.

[4] J. Vojtech, J. Radil, O. Havlis, M. Altmann, P. Skoda, and V. Smotlacha, "Resilience of semiconductor optical amplifier with holding beam injection to reflections in bidirectional reciprocal operation," in *Proc. 18th Int. Conf. Transparent Opt. Netw. (ICTON)*, Jul. 2016, pp. 1–3.

[5] R. Sundblad, "A 440 km white rabbit link using DWDM BiDi optics and a method for automated calibration of alpha and delays," presented at the 11th White Rabbit Workshop, 2021.

[6] S. M. F. Raupach, A. Koczwara, and G. Grosche, "Brillouin amplification supports $1\times10^{-20}$ uncertainty in optical frequency transfer over 1400 km of underground fiber," *Phys. Rev. A, Gen. Phys.*, vol. 92, no. 2, Aug. 2015, Art. no. 021801, doi: 10.1103/PhysRevA.92.021801.

[7] O. Havlis et al., "Bidirectional optical amplifier delivering high gain," in *Proc. Eur. Freq. Time Forum (EFTF)*, Apr. 2018, pp. 303–307.

[8] L. Rapp and M. Eiselt, "Optical amplifiers for multi–band optical transmission systems," *J. Lightw. Technol.*, vol. 40, no. 6, pp. 1579–1589, Mar. 15, 2022, doi: 10.1109/JLT.2021.3120944.

[9] M. Lipinski, T. Wlostowski, J. Serrano, and P. Alvarez, "white rabbit: A PTP application for robust sub-nanosecond synchronization," in *Proc. IEEE Int. Symp. Precis. Clock Synchronization Meas., Control Commun. (ISPCS)*, Sep. 2011, pp. 25–30.

[10] H. Peek and P. Jansweijer, "white rabbit absolute calibration," in *Proc. IEEE Int. Symp. Precis. Clock Synchronization Meas., Control, Commun. (ISPCS)*, Sep. 2018, pp. 1–5.

[11] P. P. M. Jansweijer, N. A. D. Boukadida, K. Hanhijärvi, A. Wallin, B. Eglin, and E. L. English, "First electrical white rabbit absolute calibration inter-comparison," 2022, *arXiv:2201.08640*, doi: 10.48550/arXiv.2201.08640.

[12] P. Jansweijer and H. Peek, "Insitu determination of the fiber delay coefficient in time-dissemination networks," in *Proc. IEEE Int. Symp. Precis. Clock Synchronization Meas., Control, Commun. (ISPCS)*, Sep. 2019, pp. 1–6, doi: 10.1109/ISPCS.2019.8886632.

[13] P. S. André and A. N. Pinto, "Chromatic dispersion fluctuations in optical fibers due to temperature and its effects in high-speed optical communication systems," *Opt. Commun.*, vol. 246, nos. 4–6, pp. 303–311, Feb. 2005, doi: 10.1016/j.optcom.2004.11.017.

[14] P. S. André et al., "Transmission fiber chromatic dispersion dependence on temperature: Implications on 40 Gb/s performance," *ETRI J.*, vol. 28, no. 2, pp. 257–259, Apr. 2006, doi: 10.4218/etrij.06.0205.0070.

[15] T. Fordell, "Open-loop polarization mode dispersion mitigation for fibre-optic time and frequency transfer," *Opt. Exp.*, vol. 30, no. 4, pp. 6311–6319, Feb. 2022, doi: 10.1364/OE.448553.

[16] M. Theurer et al., "2 × 56 GB/s from a double side electroabsorption modulated DFB laser and application in novel optical PAM4 generation," *J. Lightw. Technol.*, vol. 35, no. 4, pp. 706–710, Feb. 15, 2017, doi: 10.1109/JLT.2016.2597962.

[17] M. Jiménez-López, F. Girela-López, J. López-Jiménez, E. Marín-López, R. Rodríguez, and J. Díaz, "10 gigabit white rabbit: sub-nanosecond timing and data distribution," *IEEE Access*, vol. 8, pp. 92999–93010, 2020, doi: 10.1109/ACCESS.2020.2995179.

[18] Ł. Śliwczyński, P. Krehlik, Ł. Buczek, and H. Schnatz, "Synchronized laser modules with frequency offset up to 50 GHz for ultra-accurate long-distance fiber optic time transfer links," *J. Lightw. Technol.*, vol. 40, no. 9, pp. 2739–2747, May 1, 2022, doi: 10.1109/JLT.2022.3147591.

[19] E. Agrell et al., "Roadmap of optical communications," *J. Opt.*, vol. 18, no. 6, May 2016, Art. no. 063002, doi: 10.1088/2040-8978/18/6/063002.